JOURNAL OF MATERIALS SCIENCE 24 (1989) 381–388

Effects of cooling rate control during the solidification process on the microstructure and mechanical properties of cast Co–Cr–Mo alloy used for surgical implants

L. Z. ZHUANG, E. W. LANGER
Department of Metallurgy, The Technical University of Denmark, DK-2800 Lyngby, Denmark

Both dendritic structure and equiaxed grain structure are produced in cast Co–Cr–Mo alloy by control of the cooling rate of castings during the solidification process, to determine whether a significant improvement in the mechanical properties of the alloy can be obtained. The different structural characteristics of the two kinds of casting are examined by optical microscopy, scanning electron microscopy and transmission electron microscopy. Tensile and fatigue tests as well as hardness measurement are carried out using individually cast test-pieces. Fracture surface appearance characteristics of tensile and fatigue specimens are also studied. It is concluded that the mechanical properties, including both transient and permanent properties, of the equiaxed grain structure castings obtained by fast cooling are superior to those found in the coarse dendritic structure castings.

1. Introduction

A prosthetic material ideally must function mechanically without permanent deformation or failure while leaving the biological tissues completely unaltered. Therefore, the materials used for surgical implants must be resistant to corrosion by physiological fluids; strong enough to withstand without fracture the normal physiological forces, both in the short term associated with overloading and in the longer term due to fatigue, often imposed on prosthetic appliances; resistant enough to stress corrosion to withstand high stresses while in a corrosive environment; and finally they must have a high degree of biocompatibility to ensure correct healing after insertion [1–4].

Cast Co–Cr–Mo alloys have a long history of successful use as surgical implants [5] due to their outstanding corrosion resistance, wear behaviour and biocompatibility. However, a significant number of such implants have been found to fracture during implantation, excision or in service [6]. Such failures, when they occur, are important to all concerned. Consequently, premature failures in service of surgical implants inside the human body should be avoided by all means. In addition, the implant failures of cast Co–Cr–Mo alloys have raised doubts about the alloy's mechanical properties [7–12] and its low ductility and fatigue strength are now a matter of concern, especially since the introduction of newer alloys which are also used as implant appliances such as Ti–6Al–4V.

For these reasons, many efforts to improve the mechanical properties, especially the fatigue properties, of investment-cast Co–Cr–Mo alloys have been made. The use of hot isostatic pressing (HIP) processing improves the ductility and tensile properties [13–18]. The mechanical property improvements by various heat-treatment schemes have been studied comprehensively [9, 18–25]. Studies of the mechanical behaviour of hot-forged cast Co–Cr–Mo alloys have also been carried out [26, 27]. Furthermore, the effects of alloy element additions on cast Co–Cr–Mo alloys have been investigated by Cohen *et al.* [19] and by Kilner and co-workers [28, 29]. However, the results of these studies are not mutually consistent and some clear contradictions exist between these investigations. This paper deals with the improvements of microstructure and mechanical properties of cast Co–Cr–Mo surgical implant alloys by controlling the casting conditions during the solidification process.

2. Materials and experimental procedure

Cast Co–Cr–Mo alloy, commercially known as Vitallium or H.S. 21, was studied. The chemical composition of the alloy used was (in wt %): 29.15 Cr, 6.50 Mo, 0.06 Fe, 0.05 Si, 0.10 Mn, 0.16 C and balance cobalt. Individually cast specimens were used for mechanical testing. Specimens were mechanically tested and examined optically or by scanning electron microscopy as well as transmission electron microscopy in the as-cast condition.

In order to study the differences of microstructure and mechanical properties caused by control of the cooling procedure, both a sand mould with air cooling and a metallic mould with water cooling were used to obtain two different cast structures: coarse dendritic structure which is the typical casting structure observed in cast Co–Cr–Mo surgical implant alloys, and equiaxed grain structure which is a modified casting structure produced by fast cooling. Individual specimens

0022–2461/89 $03.00 + .12

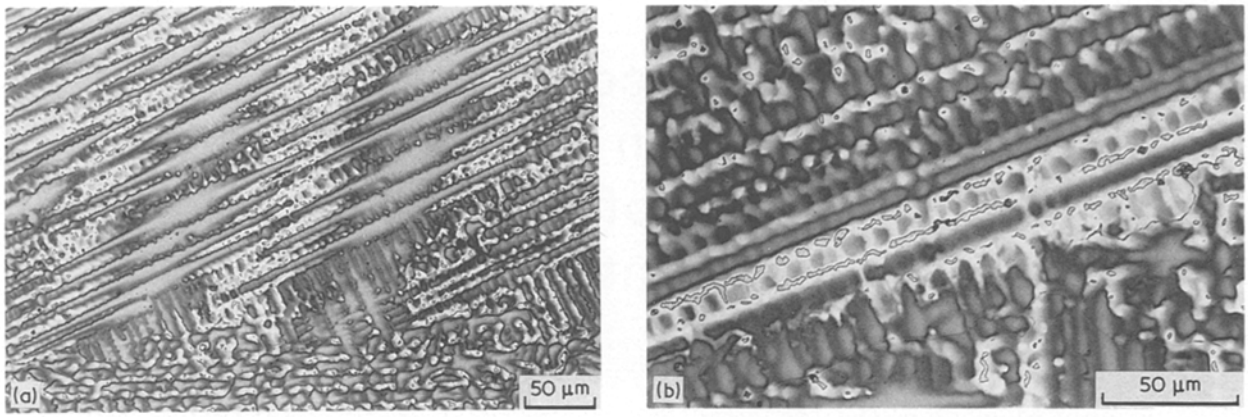

Figure 1 The outer layer structure of slowly cooled castings, showing the directional growth of dendrites and inhomogeneous distribution of carbide precipitates: (a) carbide separation in interdendrites, (b) abnormally long bands of interdendritic carbides near grain boundary. Electrolytically etched with 60% HNO_3 + 40% H_2O.

were cast with the dimension of 85 mm × 20 mm × 30 mm.

Metallographic specimens were prepared by an electrolytic etching method with etchant 60% HNO_3 + 40% distilled water by volume, 10 to 25 sec at 5 V. The extent of coring across the dendrites was measured using energy-dispersive spectrometry (EDS) microanalysis for the coarse dendritic structure cast specimens. Fresh fracture surfaces of tensile and fatigue specimens were examined in a Philips SEM505 scanning electron microscope. Transmission electron microscopy was performed using disc-shaped specimens with 3 mm diameter. Final thinning was executed using an electrolyte of 10 vol % perchloric acid + 20 vol % ethanol + 70 vol % butanol. The electrolyte temperature was maintained at −20 to −30° C throughout thinning and the operating potential was 30 V. The specimens were examined in a Philips EM301 transmission electron microscope operating at 100 kV.

Vickers microhardness measurements were made on polished surfaces using a load p = 25 g. Tensile tests were performed using an Instron testing machine (Model 1115) and a calibrated strain-gauge extensometer. Tensile test specimens were cylindrical, machined to a diameter of 6 mm from the original castings. The strain rate in the elastic region was 0.005 min^{-1}. Fatigue tests were conducted using an Instron testing machine (Model 1342) at 10 Hz and load ratio R = 0.1. Constant-load-amplitude fatigue crack growth rates [30] were determined using standard three-point bend specimens [31] with S = 64 mm, W = 16 mm, B = 8 mm and total specimen length L = 80 mm. A 3 mm notch was made using spark-cutting in advance and fatigue precracking of the test specimens was carried out in the same fixtures in which they were fatigue-tested.

3. Results and discussion

3.1. Microstructure analysis

The as-cast alloy obtained using a sand mould with air cooling exhibits the typical microstructure, as shown in Figs 1 and 2, namely a cored cobalt-rich face-centred cubic matrix with interdendritic carbides and grain boundary precipitates. Fig. 1 shows the outer layer structure of castings in which the directional growth of dendritic structure and a seriously inhomogeneous distribution of interdendritic carbide precipitates are clearly observed. A coarser dendritic structure with random growth directions and a more homogeneous distribution of carbides can be seen in the centre part of the castings, as shown in Fig. 2. The as-cast alloy obtained using a metallic mould with water cooling (fast cooling) shows an equiaxed grain structure, as shown in Fig. 3. Most of the carbide precipitates are located at the grain boundaries so that continuous grain boundary carbide precipitations are formed. Therefore, carbides precipitated inside grains

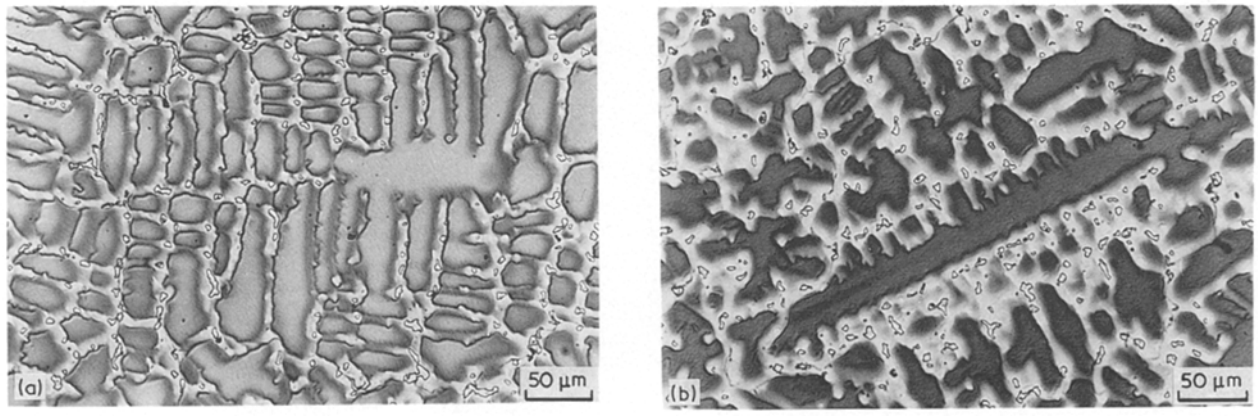

Figure 2 (a, b) Structure of the centre parts of slowly cooled castings showing larger, randomly grown dendrites and a homogeneous distribution of interdendritic carbides. Electrolytically etched with 60% HNO_3 + 40% H_2O.

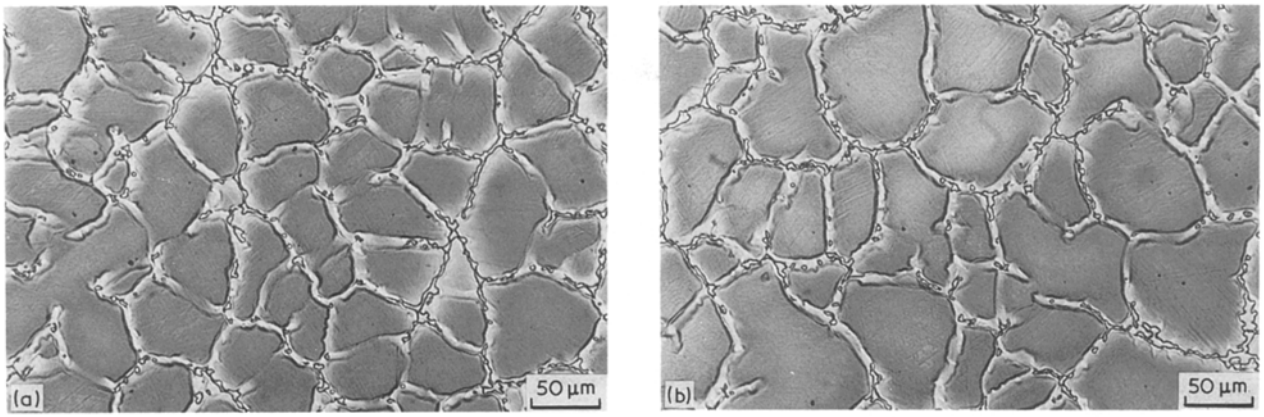

Figure 3 Cast Co–Cr–Mo alloy obtained by using a metallic mould with water cooling, showing the equiaxed grain structure and grain boundary carbide precipitations: (a) fine equiaxed grains adjacent to the thin layer of dendrites formed in the outermost region of the castings, (b) structure of the centre part of the casting. Electrolytically etched with 60% HNO_3 + 40% H_2O.

are seldom observed in equiaxed grain-structure alloy. There is only a thin layer of directionally grown dendritic structure which is removed during the machining of the mechanical testing specimens in the fast-cooled cast alloy. Fine equiaxed grains adjacent to the thin layer of dendrites are formed, as in Fig. 3a. Both in the slowly cooled castings and in the fast-solidified casting, the grain size of the centre part of the castings is larger than in the outer region.

Comparing the microstructures shown in Figs 1 to 3, it is easy to list the following differences between these two cast alloys.

(a) The slowly cooled cast alloy has a coarse dendritic structure while the fast-cooled cast alloy shows a nearly completely fine equiaxed grain structure. The average grain sizes (average grain number per millimetre length) are $\bar{g} = 2.6$ and $16.0\,mm^{-1}$, respectively.

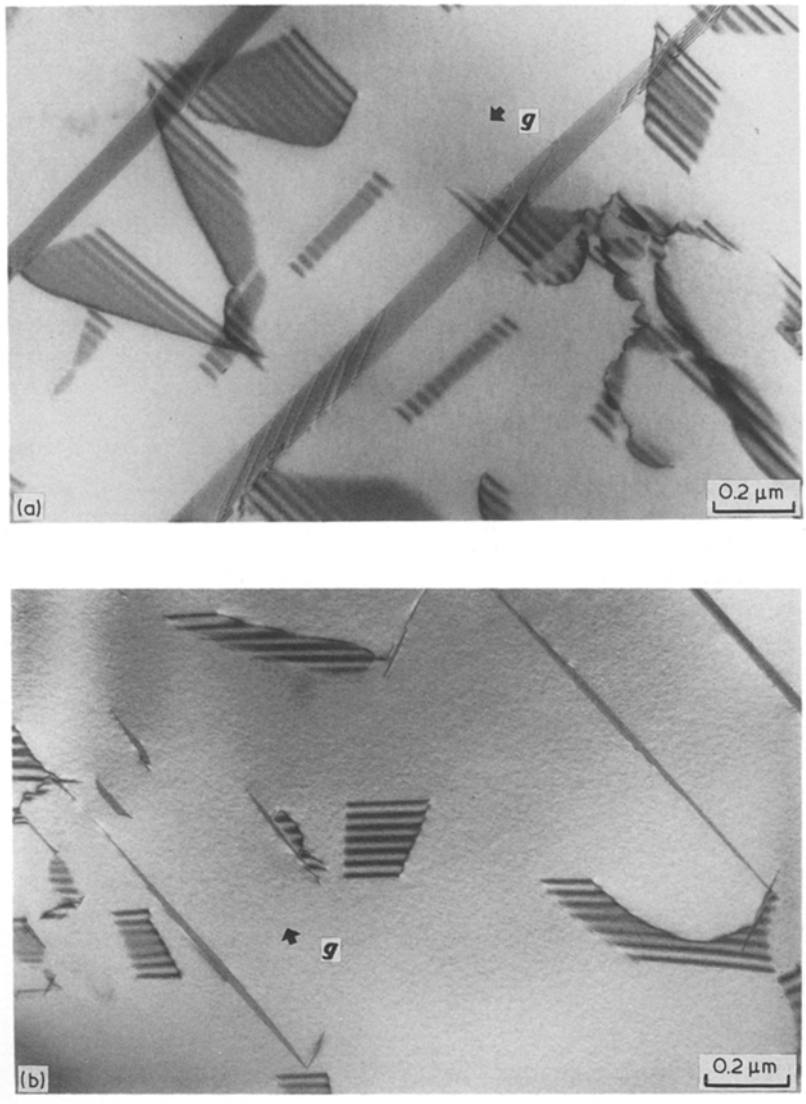

Figure 4 TEM micrographs showing the structure of dissociated dislocations and stacking-fault bands in cast Co–Cr–Mo alloys: (a) fast-cooled cast alloy, $\boldsymbol{g} = [2\,0\,0]$; (b) slowly cooled cast alloy, $\boldsymbol{g} = [\bar{1}\,1\,\bar{1}]$.

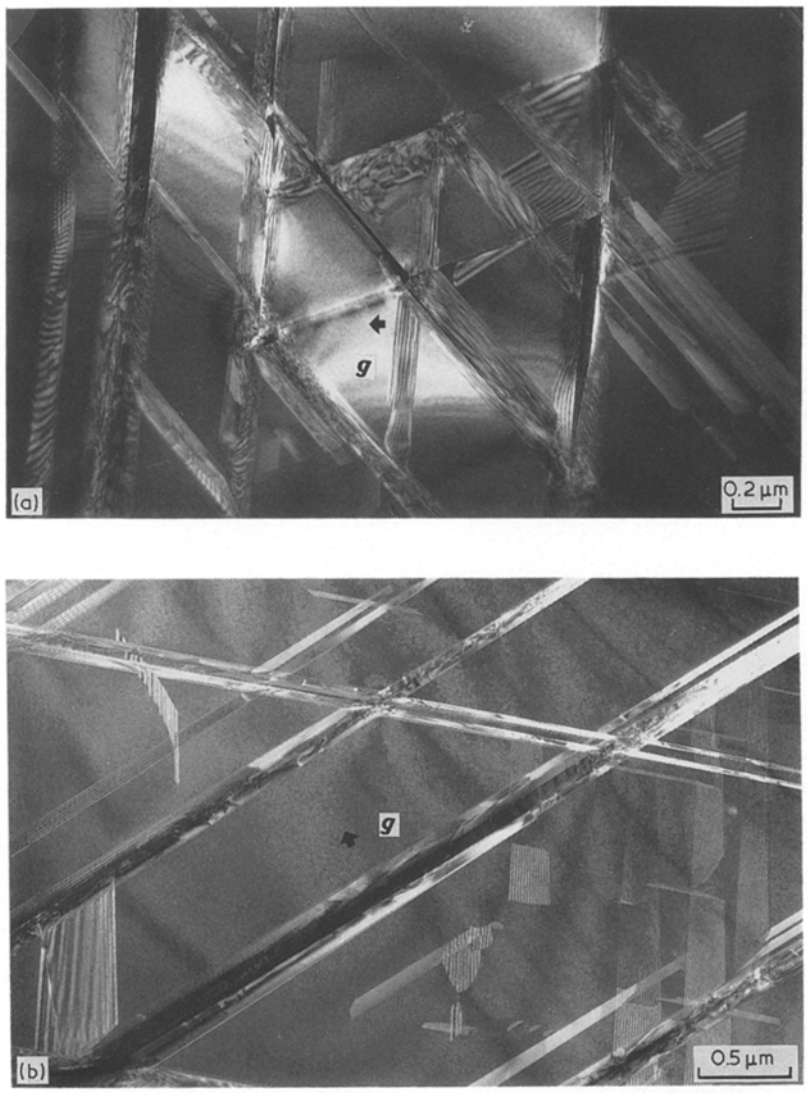

Figure 5 Dark-field TEM micrographs showing fcc stacking faults and stacking fault intersections in cast Co–Cr–Mo alloys: (a) fast-cooled cast alloy, $\boldsymbol{g}$ = [2 2 0]; (b) slowly cooled cast alloy, $\boldsymbol{g}$ = [1 1 1].

(b) In the slowly cooled castings, most of the carbides are precipitated in the interdendritic regions and an inhomogeneous distribution of interdendritic carbides is observed. There is almost no grain boundary carbide precipitation in this kind of cast alloy. In the fast-cooled castings, however, most of the carbides are precipitated at grain boundaries and the continuous grain boundary carbide precipitations are observed easily. There are few carbide precipitates inside the grain crystals.

(c) EDS microanalysis results confirm that the principal elements exhibit segregation in the slowly cooled cast alloy because of the presence of coarse dendritic structure. The extent of coring across the dendrites for molybdenum is about 9 wt % in the dendrites and 4.5 wt % in the interdendritic regions, and for chromium 32 wt % in the dendrites and 27 wt % in the interdendritic regions. In the fast-cooled cast alloy however, element segregations in the equiaxed grain crystals have not been observed.

Microstructures produced in the Co–Cr–Mo alloy were examined by transmission electron microscopy in both fast and slowly cooled specimens. In all cases, it is found that a considerable formation of dissociated dislocations combined with fcc stacking faults and twins exists in the Co–Cr–Mo alloys in the as-cast state. However, a higher density of these fine defect structures is observed in the fast-cooled cast alloy, presumably because higher stresses or strains were developed here than in the slowly cooled cast alloy during solidification. Typical TEM microstructures are shown in Figs 4 to 6. These microstructural characteristics are mainly determined by the fact that this alloy has a very low stacking-fault energy. Also this microstructural information can be successfully used to explain the observed tensile and fatigue fracture behaviour of this cast surgical implant alloy.

3.2. Mechanical behaviour

The results of tensile tests and Vickers microhardness measurements for the alloys produced by two different solidification procedures, compared to the ASTM standards, are listed in Table I. It is obvious that the

TABLE I Tensile properties and hardness of cast Co–Cr–Mo alloys

Condition	YS* (MPa)	UTS (MPa)	Elongation (%)	Hardness
As-cast ASTM Spec. F75–76	450	655	8.0	25 to 35 HRC
As-cast slowly cooled H.S.21	523	739	6.6	322 HV
As-cast fast-cooled H.S.21	578	954	11.8	356 HV

*0.2% offset.

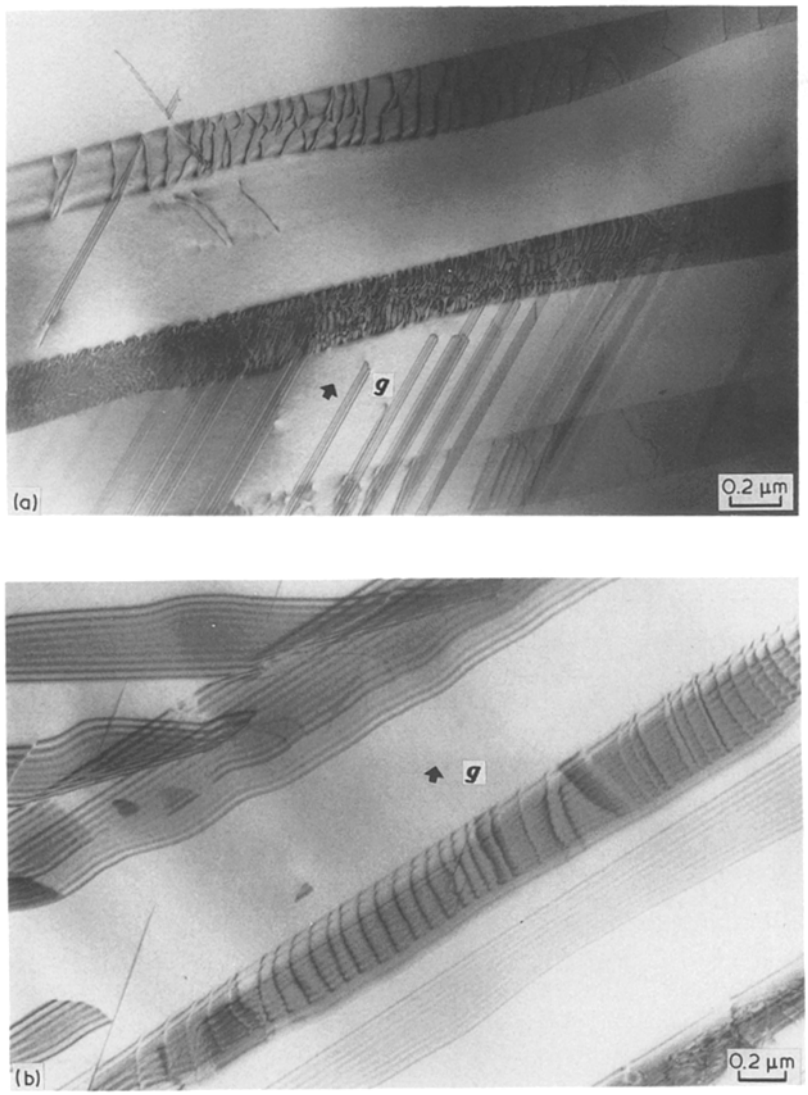

Figure 6 Detailed views of dislocation pile-ups in the stacking faults and the interaction of stacking faults in cast Co–Cr–Mo alloys: (a) fast-cooled cast alloy; $g = [2\bar{2}0]$, (b) slowly cooled cast alloy, $g = [00\bar{2}]$.

fast-cooled cast alloy which has the equiaxed grain structure has better mechanical properties, both in strength and ductility. SEM micrographs of tensile fracture surfaces for these two cast alloys are shown in Figs 7 and 8. The appearances of the fracture surfaces are quite different. The slowly cooled cast alloy shows a mixture of fracture modes and fractures along the dendrites, while the fast-cooled cast alloy exhibits a ductile fracture characteristic.

The tensile strength and hardness of the alloy can be related to the grain size, compositional homogeneity in the matrix, the amount and morphology as well as distribution of minor phases (particularly carbides in this alloy), dislocation and stacking-fault densities and distributions, etc. Slip in the fcc phase will be restricted by the presence of stacking-fault bands and by the existence of twins. As the density of stacking faults and twins increases, the mean free slip path will decrease and a higher strength is expected. The results presented demonstrate that the fast-cooled cast alloy has a fine equiaxed grain structure and a very homogeneous matrix which are favourable factors for the improvement of the alloy's mechanical properties. Furthermore, fast solidification increases the density of fcc stacking faults, twins and dissociated dislocations, thus rationalizing in terms of the fcc slip

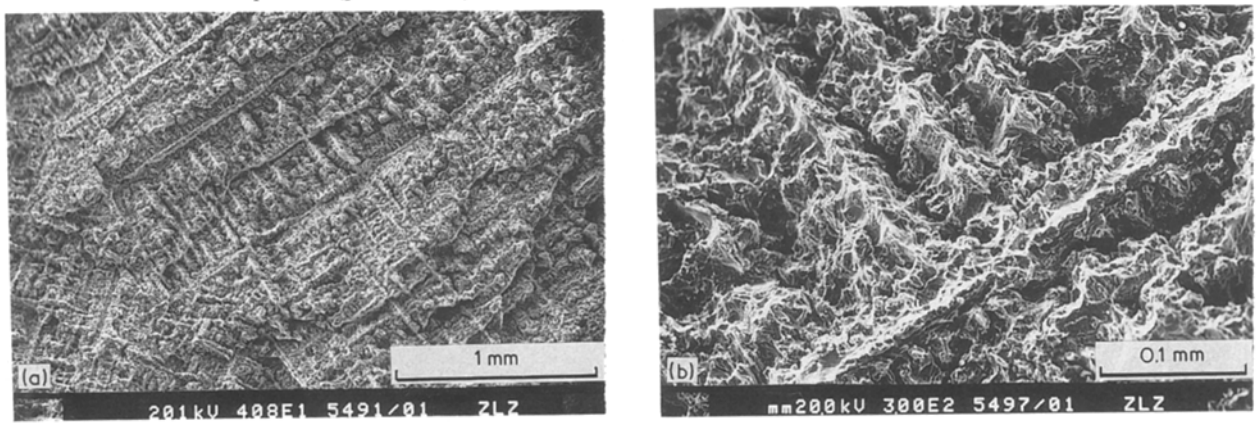

Figure 7 (a, b) SEM micrographs showing the tensile fracture appearance of the dendritic structure in cast Co–Cr–Mo alloy.

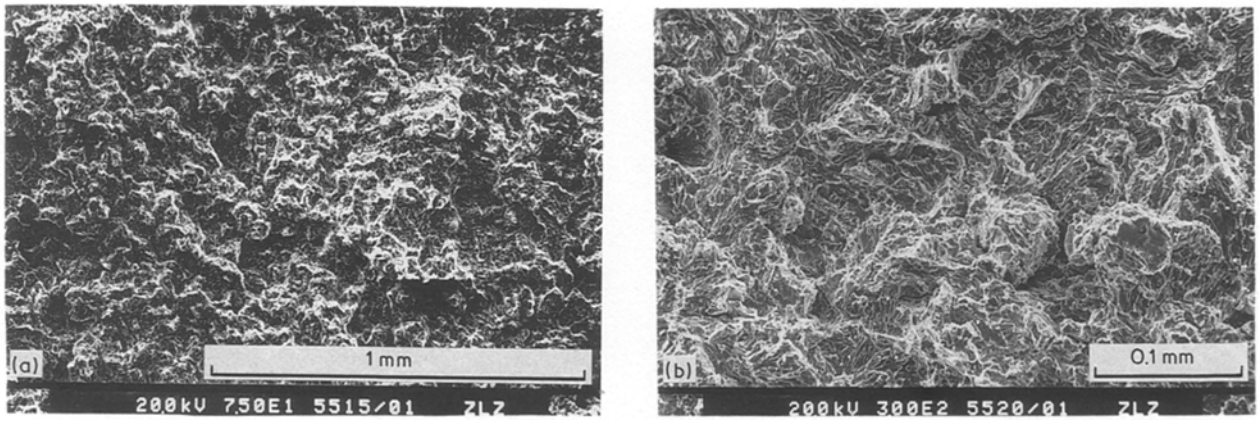

Figure 8 (a, b) SEM micrographs showing the tensile fracture appearance of the equiaxed grain structure in cast Co–Cr–Mo alloy.

mechanism the improvement in mechanical properties observed. A significant difference in tensile ductility between the two cast alloys is mainly caused by the differences of structural characteristics: a coarse and inhomogeneous dendritic structure in slowly cooled cast alloy and a fine and homogeneous equiaxed grain structure in fast-cooled cast alloy.

Fracture mechanics concepts have been applied successfully to crack growth during cyclic loading in fcc, bcc and hcp structured materials as shown by Paris and Erdogan [32, 33]:

$$da/dN = C(\Delta K)^n \quad (1)$$

where ΔK is the range of stress intensity factor during a fatigue cycle, i.e. $\Delta K = K_{max} - K_{min}$; C and n are assumed to be material constants which have been shown to depend on the mean load [34–36]. Values of the exponent n, which is the slope of the crack-growth-rate curve based on Equation 1, have been found to lie mainly in the range 2 to 4; however, there is some evidence that in medium- and high-strength steels much higher values (up to 10) can be obtained, particularly in steels with a low fracture toughness [37–39].

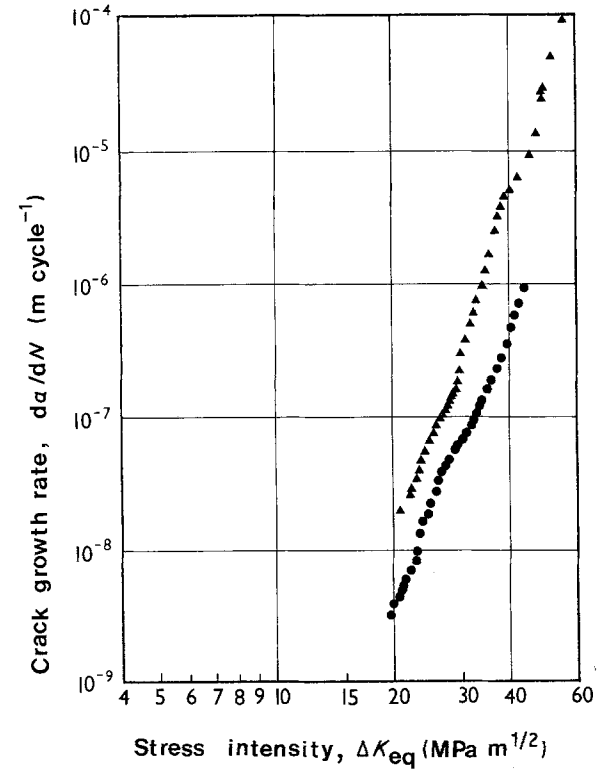

Figure 9 Fatigue crack propagation behaviour in cast Co–Cr–Mo alloy showing the effect of cast structure on crack growth rate at constant amplitude: (▲) dendritic structure, (●) equiaxed grain structure.

The data shown in Fig. 9 indicate the influence of cast structure on the fatigue crack propagation behaviour in cast Co–Cr–Mo alloys. The crack growth rate of dendritic structure alloy is faster than that of equiaxed grain structure alloy for the same ΔK values, and the crack growth rate of dendritic structure cast alloy increases faster than that of equiaxed grain structure cast alloy with increasing ΔK values. Regression equations of fatigue crack growth rate for these two alloys using Equation 1 are shown in Table II. Note that an excellent correlation exists between the stress intensity factor range and the fatigue crack growth rates in the alloys tested. The values of n for cast Co–Cr–Mo alloys are much higher than that found in most conventional alloys: 8.7 and 6.7 for dendritic structure cast alloy and equiaxed grain structure cast alloy, respectively, corresponding to stress intensity factor range between 20 and 50 MPa $m^{1/2}$. The reason why the cast Co–Cr–Mo alloys have higher values of n is probably because of their low ductility.

Examination of the fatigue fracture surface appearances proves that the fatigue cracks propagate with an identical mechanism in the two cast alloys. Both SEM and optical micrographs reveal that the fatigue cracks propagate on special crystallographic planes so that faceted fatigue fracture surfaces are formed. Figs 10 and 11 show the SEM micrographs of fatigue fracture appearances of dendritic structure cast alloy and equiaxed grain structure alloy, respectively. In these figures, it is shown that the fractures are very brittle and with no signs of fatigue striations. The four different $\{1\,1\,1\}_{fcc}$ plane orientations can be discerned in the SEM micrographs. In fcc structure materials the dominant slip systems are $\{1\,1\,1\}\langle 1\,\bar{1}\,0\rangle$, i.e. in fcc

TABLE II Regression equations of fatigue crack growth rate for cast Co–Cr–Mo alloys

Alloy*	Equation	Interrelation factor, R
D	$da/dN = 4.026 \times 10^{-20}(\Delta K)^{8.7}$	0.993
E	$da/dN = 7.312 \times 10^{-18}(\Delta K)^{6.7}$	0.996

*D = dendritic structure, E = equiaxed grain structure.

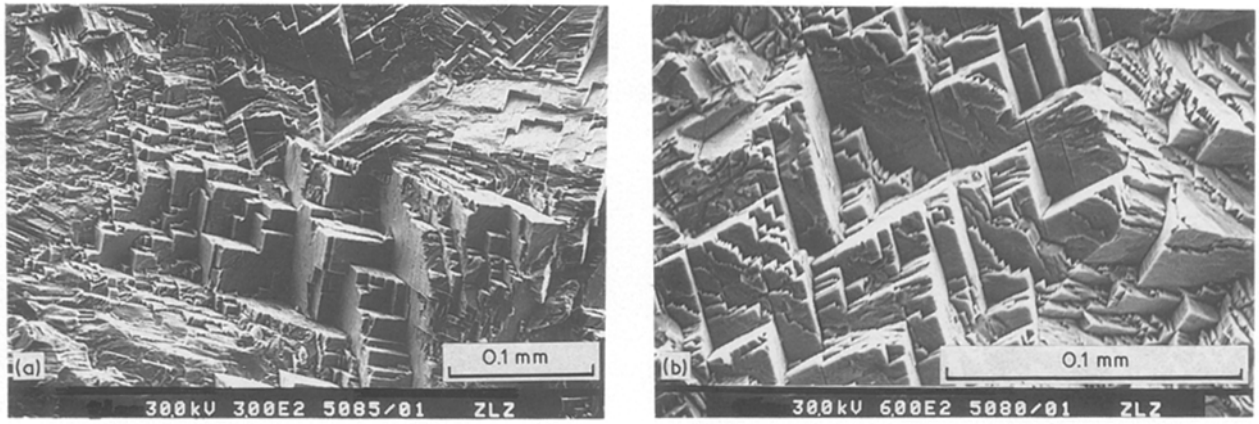

Figure 10 (a, b) SEM micrographs showing the fatigue fracture appearance of coarse dendritic structure cast Co–Cr–Mo alloy. Faceted growth and stepwise cleavage fractures following crystallographic planes.

crystals, slip occurs most often on {1 1 1} octahedral planes and in $\langle 1\,\bar{1}\,0 \rangle$ directions which are parallel to cubic face diagonals, according to the theory of the deformation mechanism. SEM observation indicates that the fracture surfaces of cast Co–Cr–Mo alloys have typical {1 1 1} slip-plane faceted fracture characteristics showing the 60° angle between different {1 1 1} crystal planes. The fracture surfaces are seen to consist of zigzag segments and a block structure with steps. Polished and etched side views, of the fracture surfaces are shown in Fig. 12. It is apparent that the crack growth is associated preferentially with specific crystallographic planes, i.e. {1 1 1} planes, in both cast alloys.

It is known that the conditions favouring faceted fractures are (a) a coarse grain size and (b) low stress levels with respect to the yield stress and (c) a low stacking fault energy [40-42].

The Co–Cr–Mo alloy has a very low stacking-fault energy which facilitates the formation of dense stacking faults and twins, as shown in TEM micrographs. The presence of dense stacking faults and twins can affect the fatigue fracture behaviour significantly. These will be studied separately in another paper. Well-developed facets are observed on the fracture surfaces of slowly cooled cast alloy which has a coarse dendritic structure, shown in Fig. 10.

The improvement of fatigue properties, as shown in Fig. 9, by fast cooling mainly comes from the improvement of the cast structure. The fine and homogeneous equiaxed grain structure provides a higher resistance to fatigue crack propagation than the coarse and inhomogeneous dendritic structure. It is believed that a fatigue crack propagates preferentially in the dendritic regions where shrinkage cavities are often found.

4. Conclusions

1. By the control of the solidification process of casting, both coarse dendritic structure and fine equiaxed grain structure can be obtained in cast Co–Cr–Mo alloys. TEM microstructure observations reveal that these two cast alloys have the same fine microstructural characteristics: dense dissociated dislocations combined with fcc stacking faults and twins. These characteristics are determined by the chemical composition of the matrix.

2. The fine equiaxed grain structure cast alloy improves both transient and permanent mechanical properties markedly. The fatigue behaviour of the two cast alloys can be expressed as: $da/dN = 4.026 \times 10^{-20} (\Delta(K))^{8.7}$ for dendritic structure cast alloy and $da/dN = 7.312 \times 10^{-18} (\Delta(K))^{6.7}$ for equiaxed grain structure cast alloy within the stress intensity factor range between 20 and 50 MPa $m^{1/2}$.

3. Faceted fatigue fracture surfaces are observed in cast Co–Cr–Mo alloy. Low stacking-fault energy of the alloy is considered as one of the main factors

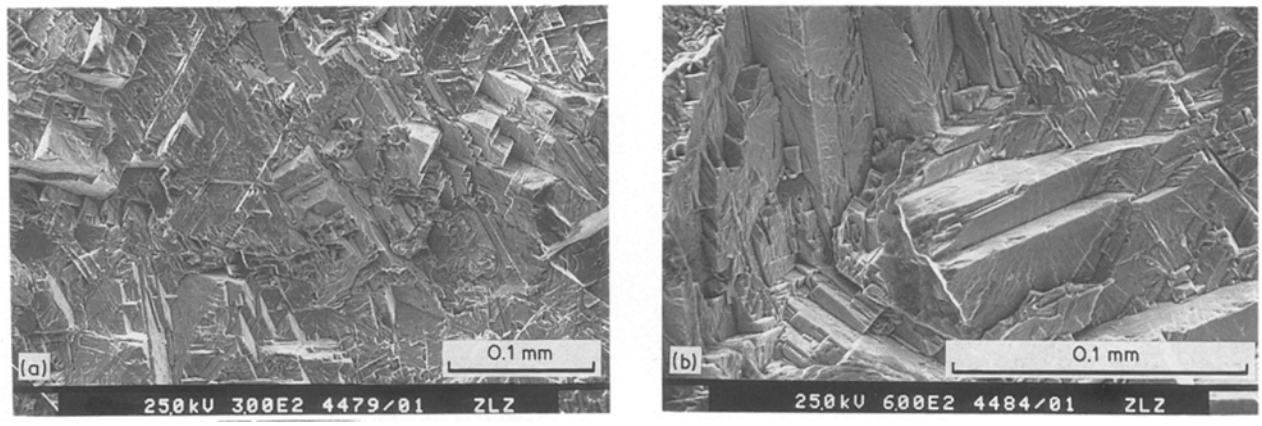

Figure 11 (a, b) SEM micrographs showing the fatigue fracture appearance of equiaxed grain structure cast Co–Cr–Mo alloy. Faceted growth and stepwise cleavage fractures following crystallographic planes.

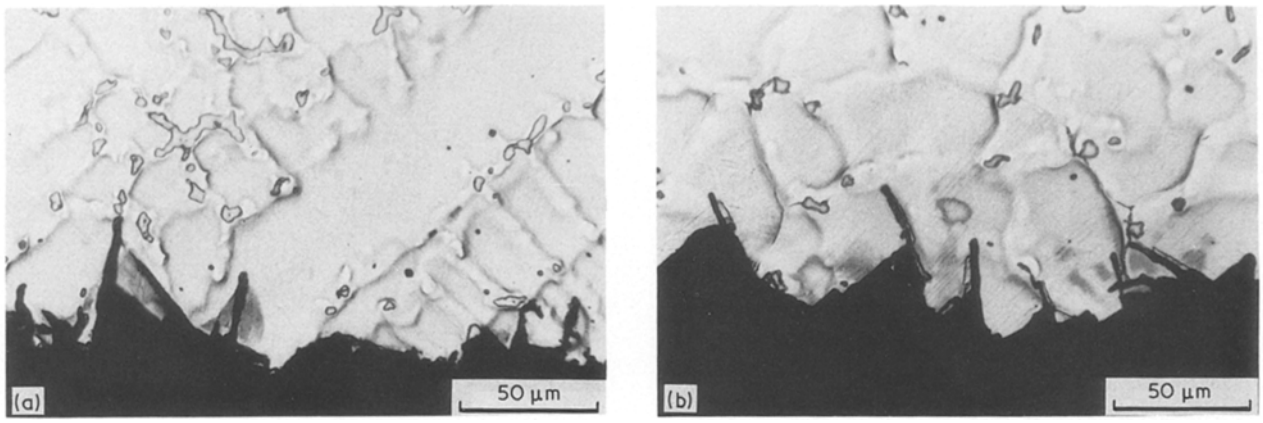

Figure 12 Optical micrographs showing fatigue crack propagation following special crystallographic planes in cast Co–Cr–Mo alloys: (a) dendritic structure cast alloy, (b) equiaxed grain structure cast alloy. Electrolytically etched with 60% HNO_3 + 40% H_2O.

which dominate the appearance of the fatigue fracture surfaces. Well-developed facets are observed on the fracture surfaces of dendritic structure cast alloy which are attributed to its larger grain size.

Acknowledgements

The authors would like to express their gratitude to Dr P. Brøndsted, Metallurgy Department, Risø National Laboratory, who helped them to perform the tensile and fatigue testings in his department. They are also grateful to the staff of the department for experimental help, especially to Mrs A. Steffensen who printed the photographs.

References

1. D. C. MEARS, *Int. Metals Rev.* **22** (1977) 119.
2. D. S. CRIMMINS, *J. Metals* **21** (1969) 38.
3. J. COHEN, *J. Mater. Sci.* **1** (1966) 354.
4. W. BONFIELD, *Metals Mater.* **3** (1987) 712.
5. F. R. MORRAL, *J. Mater. Sci.* **1** (1966) 384.
6. J. T. SCALES, *J. Bone Joint Surg.* **53B** (1972) 344.
7. N. D. GREENE, C. ONKELINX, L. J. RICHELLE and P. A. WARD, in Proceedings of Biomaterials Symposium, New Orleans, April 1974, edited by E. Horowitz and J. L. Torgesen, Institute for Materials Research (National Bureau of Standards, Washington, 1975) p. 45.
8. M. F. SEMLITSCH, B. PANIC, H. WEBER and R. SCHOEN, ASTM STP 796 (American Society for Testing and Materials, Philadelphia, 1983) p. 120.
9. A. J. T. CLEMOW and B. L. DANIELL, *J. Biomed. Mater. Res.* **13** (1979) 265.
10. P. DUCHEYNE, P. DEMEESTER, E. AERNOUDT, M. MARTENS and J. C. MULIER, *J. Biomed. Mater. Res. Symp.* **6** (1975) 199.
11. E. SMETHURST and R. B. WATERHOUSE, *J. Bone Joint Surg.* **58B** (1976) 372.
12. J. O. GALANTE, W. ROSTOKER and J. M. DOYLE, *ibid.* **57A** (1975) 2.
13. F. G. HODGE and T. S. LEE, *Corrosion* **31** (1975) 111.
14. T. M. DEVINE and J. WULFF, *J. Biomed. Mater. Res.* **9** (1975) 151.
15. R. HOLLANDER and J. WULFF, *Metals Eng. Quart.* **14**(4) (1974) 37.
16. *Idem, J. Biomed. Mater. Res.* **9** (1975) 367.
17. H. A. LUCKEY and L. J. BARNARD, in Mechanical Properties of Biomaterials, edited by G. W. Hastings and D. F. Williams (John Wiley, Chichester, 1980) p. 311.
18. R. HOLLANDER and J. WULFF, *Eng. Med.* **3** (1974) 8.
19. J. COHEN, R. M. ROSE and J. WULFF, *J. Biomed. Mater. Res.* **12** (1978) 935.
20. M. LORENTZ, M. SEMLITSCH, B. PANIC, H. WEBER and H. G. WILLERT, *Eng. Med.* **7** (1978) 241.
21. J. B. VANDER SANDE, J. R. COKE and J. WULFF, *Met. Trans.* **7A** (1976) 389.
22. H. S. DOBBS and J. L. M. ROBERTSON, *J. Mater. Sci.* **18** (1983) 391.
23. K. RAJAN, *Met. Trans.* **13A** (1982) 1161.
24. R. N. J. TAYLOR and R. B. WATERHOUSE, *J. Mater. Sci.* **18** (1983) 3265.
25. *Idem, ibid.* **21** (1986) 1990.
26. T. M. DEVINE, F. J. KUMMER and J. WULFF, *ibid.* **7** (1972) 126.
27. J. P. IMMARIGEON, K. RAJAN and W. WALLACE, *Met. Trans.* **15A** (1984) 339.
28. T. KILNER, A. J. DEMPSEY, R. M. PILLIAR and G. C. WEATHERLY, *J. Mater. Sci.* **22** (1987) 565.
29. A. J. DEMPSEY, R. M. PILLIAR, G. C. WEATHERLY and T. KILNER, *ibid.* **22** (1987) 575.
30. Annual Book of ASTM Standards, Part 10, E647-81 (American Society for Testing and Materials, Philadelphia, 1981) p. 765.
31. *Idem*, E399-81 (1981) p. 588.
32. P. C. PARIS and F. ERDOGAN, *Trans. ASME Series D* **85** (1963) 528.
33. P. C. PARIS, "Fatigue – An Interdisciplinary Approach" (Syracuse University Press, Syracuse, 1964) p. 107.
34. W. J. MILLS and R. W. HERTZBERG, ASTM STP 569 (American Society for Testing and Materials, Philadelphia, 1975) p. 5.
35. L. P. POOK, ASTM STP 513 (American Society for Testing and Materials, Philadelphia, 1972) p. 106.
36. R. O. RITCHIE and J. F. KNOTT, *Acta Metall.* **21** (1973) 639.
37. G. A. MILLER, *Trans. ASM* **61** (1968) 442.
38. W. G. CLARK and E. T. WESSEL, ASTM STP 463 (American Society for Testing and Materials, Philadelphia, 1970) p. 106.
39. P. R. V. EVANS, N. B. OWEN and B. E. HOPKINS, *Eng. Fract. Mech.* **3** (1971) 463.
40. C. E. PRICE, *Metallography* **17** (1984) 359.
41. R. W. HERTZBERG and W. J. MILLS, ASTM STP 600 (American Society for Testing and Materials, Philadelphia, 1976) p. 220.
42. C. E. PRICE and R. KUNC, *Metallography* **19** (1986) 317.

Received 27 January
and accepted 20 May 1988